IEEE Access
Multidisciplinary ⋮ Rapid Review ⋮ Open Access Journal

Received 22 May 2022, accepted 27 June 2022, date of publication 11 July 2022, date of current version 19 August 2022.

Digital Object Identifier 10.1109/ACCESS.2022.3189658

RESEARCH ARTICLE

H-Shaped Eight-Element Dual-Band MIMO Antenna for Sub-6 GHz 5G Smartphone Applications

MUHAMMAD NOAMAN ZAHID[1], ZHU GAOFENG[1], SAAD HASSAN KIANI[2], (Graduate Student Member, IEEE), UMAIR RAFIQUE[3], (Graduate Student Member, IEEE), SYED MUZAHIR ABBAS[4], (Senior Member, IEEE), MOHAMMAD ALIBAKHSHIKENARI[5], (Member, IEEE), AND MARIANA DALARSSON[6], (Member, IEEE)

[1]School of Information, Hunan University of Humanities, Science and Technology, Loudi 417000, China
[2]Department of Electrical Engineering, IIC University of Technology, Phnom Penh 121206, Cambodia
[3]Department of Information Engineering, Electronics and Telecommunication, Sapienza University of Rome, 00184 Rome, Italy
[4]Faculty of Science and Engineering, School of Engineering, Macquarie University, Sydney, NSW 2109, Australia
[5]Department of Signal Theory and Communications, Universidad Carlos III de Madrid, 28911 Leganés, Madrid, Spain
[6]School of Electrical Engineering and Computer Science, KTH Royal Institute of Technology, 100-44 Stockholm, Sweden

Corresponding authors: Zhu Gaofeng (hnrkzgf@163.com), Mohammad Alibakhshikenari (mohammad.alibakhshikenari@uc3m.es), and Mariana Dalarsson (mardal@kth.se)

Dr. Mohammad Alibakhshikenari acknowledges support from the CONEX-Plus programme funded by Universidad Carlos III de Madrid and the European Union's Horizon 2020 research and innovation programme under the Marie Sklodowska-Curie grant agreement No. 801538.

ABSTRACT The design of an eight-element H-shaped dual-band multiple-input multiple-output (MIMO) antenna system for sub-6 GHz fifth-generation (5G) smartphone applications is presented in this work. The radiating elements are designed on the side edge frame of the smartphone, placed on both sides of the main printed circuit board (PCB). Each side edge consists of four radiating elements, which ensures low mutual coupling between antenna elements. The total size of the main PCB is 150×75 mm^2, while the size of the side edge frame is 150×7 mm^2. A single antenna consists of an H-shaped radiating element fed using a 50Ω microstrip feeding line designed on the main board of the smartphone. The results show that, according to −6 dB impedance bandwidth criteria, the designed MIMO antenna radiates at two different frequency ranges within the allocated 5G spectrums, i.e., 3.1-3.78 GHz and 5.43-6.21 GHz with 680 MHz and 780 MHz bandwidths, respectively. It is also observed that the antenna elements are able to provide pattern diversity for both the frequency bands. Furthermore, an isolation of >12 dB is observed between any two given radiating elements. Numerous MIMO critical performance characteristics are assessed, including diversity gain (DG), envelope correlation coefficient (ECC), and channel capacity (CC). A prototype is built, measured, and it is observed that the measured and simulated data correspond well. On the basis of performance characteristics, it can be claimed that the suggested MIMO system may be used in 5G communication networks.

INDEX TERMS Dual-band, eight-element, MIMO, sub-6 GHz, side edge frame.

I. INTRODUCTION

Fifth-generation (5G) cellular networks are considered to be a viable alternative for overcoming current communication technology limitations [1]–[4]. The millimeter-wave (mm-wave) spectrum (24 GHz, 28 GHz, 37–39 GHz, and 60 GHz) has been recommended by the Federal Communications Commission (FCC) as the operational spectrum for 5G communication. However, the proposed spectrum has issues and flaws in terms of propagation, which could have an impact on network implementation. As a result, the 5G mid-band has been designated by the International Telecommunication Union (ITU) for broadband cellular communication systems. The sub-6 GHz band, commonly

The associate editor coordinating the review of this manuscript and approving it for publication was Shah Nawaz Burokur.

known as the 5G mid-band, can provide more coverage over a larger area while minimizing propagation losses. The 5G mm-wave frequency bands are ideal for dense 5G small-cell networks in metropolitan regions with increased capacity demands, as well as macro-cells that give more coverage. To accommodate a considerable volume of traffic at a high data rate, 5G services require roughly 100 MHz of bandwidth in the sub-6 GHz spectrum and 1 GHz of bandwidth in the mm-wave band. In addition, a multiple-input multiple-output (MIMO) antenna system for 5G communication systems is required to fulfill the requirements of high data rate and increased channel capacity (CC).

Li *et al.* [5] designed a 10-port dual-band MIMO antenna configuration for 3.5 GHz and 5.5 GHz mobile phone applications. They utilized a T-shaped resonator to realize a single radiating element. An L-shaped microstrip feeding line was utilized for the excitation of the radiating element. The presented results show that the isolation between closely spaced radiating elements is >10 dB. They also presented an 8-port MIMO antenna in [6] for the 3.5 GHz frequency spectrum. In this design, a fork-shaped radiating element was used instead of the T-shaped resonator. Although the isolation between antenna elements is high, it suffers from poor antenna efficiency. In [7], orthogonal mode MIMO antennas were designed for smartphone applications. The MIMO's single antenna element consisted of a pair of curved monopoles and an edge-fed dipole. The results show that the utilization of orthogonal mode configuration tends to achieve high isolation without using an additional decoupling network. Moreover, the efficiencies of the designed MIMO antennas varied in a range of 51.7-84.5% and 49-72.9%, respectively. The same type of configuration was represented in [8]. In these designs, a common grounding branch was designed between the antenna elements to act as a decoupler.

Zhang *et al.* [9] designed an 8-port MIMO antenna for wideband sub-6 GHz services. The single radiation element was composed of a 50Ω feed line, an open-circuit stub, a U-slot on the ground plane, and a slot on the side-edge. The authors observed that the designed antenna offered a wideband response from 3.3 GHz to 6 GHz. In [10], an eight-element dual-band monopole slot MIMO antenna design was presented for 5G services. They utilized the same feeding technique as presented in [5] and [6]. For 3.5 GHz 5G smartphone applications, Jiang *et al.* [11] developed a MIMO antenna system using an L-shaped coupled antenna element and a U-shaped loop antenna. To improve the isolation between the antenna elements, a neutralization line and an inverted I-slot were designed between the antennas. In [12], an L-shaped microstrip line-fed dual-polarized diamond slot MIMO antenna was designed for 5G MIMO applications. The authors demonstrated that the orthogonal arrangement of feed lines led to achieving both polarization and pattern diversity with an isolation of more than 20 dB between radiation elements. They also designed a multiband MIMO antenna configuration in [13] for sub-6 GHz services. In this design, a ring slot was etched onto the ground plane and excited with orthogonally arranged fork-shaped feed lines.

In [14], an 8-port self-isolating MIMO antenna for the 3.5 GHz frequency band was designed. A T-shaped and inverted U-shaped radiating structures connected to the ground plane were used to achieve resonance for the 3.5 GHz frequency band. To minimize antenna dimensions, two vertical stubs were inserted in the main radiating element. This type of configuration was shown to provide $\geq$20 dB of isolation. The same type of configuration was presented in [15]–[17]. In [18], a uni-planar cellular MIMO loop antenna was designed and presented for sub-6 GHz applications. The antenna elements were arranged in such a way that they provide polarization and pattern diversity in the band of interest. For improved isolation, an arrow-shaped strip was designed between the antenna elements to improve isolation. A similar MIMO antenna design was shown in [19]. A multimode planar inverted-F antenna (PIFA) was used instead of a loop-shaped element. The designed MIMO antenna provides resonance in three different frequency bands, i.e., 2.5-2.7 GHz, 3.43-3.75 GHz, and 5.6-6 GHz. In [20] and [21], a co-planar waveguide (CPW)-fed MIMO antennas were designed for sub-6 GHz 5G communication systems. The authors demonstrated that the use of the CPW technique led to achieving enhanced isolation in the operating bandwidth.

This paper presents the design of an eight-element dual-band MIMO antenna for cell phone applications. To make room for other components of the cell phone, the radiating elements are designed on the side edge frame of the cell phone board. It is found that the MIMO antennas perform well in the 3.5 GHz and 5.8 GHz frequency bands and also provide pattern diversity. The isolation between the antenna elements is >12 dB, resulting in a low envelope correlation coefficient (ECC) and high CC.

II. ANTENNA DESIGN

A. SINGLE ELEMENT DESIGN

Figure 1 shows the design of a single antenna. From the figure, it can be seen that an H-shaped radiating element was chosen for a single antenna design. It is printed on a 0.8 mm thick FR-4 substrate with a relative permittivity of 4.4. Please note that the antenna element is etched on the side edge frame of the smartphone. A coaxially fed 50Ω microstrip line is used to excite the radiating element, which is located on the main printed circuit board (PCB). The overall dimensions of the single antenna element are: $L_1 = 18$, $L_2 = 18$, $L_3 = 3$, $L_4 = 3.5$, and $W_1 = 2.5$ (all dimensions in mm).

The construction of the proposed radiating element is divided into two parts. First, the bottom part of the radiating element is designed, whose dimensions are noted to be L_1 and L_3, as shown in the inset of Figure 2. It is observed from the result of Figure 2 that the bottom narrow strip provides resonance at a 5.8 GHz frequency band (black curve). In the second and last step, a stub and another narrow strip are added

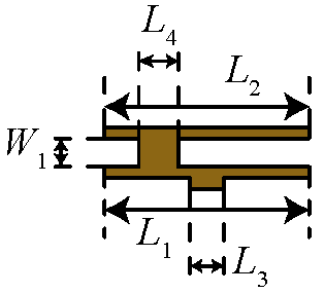

FIGURE 1. The proposed single antenna element.

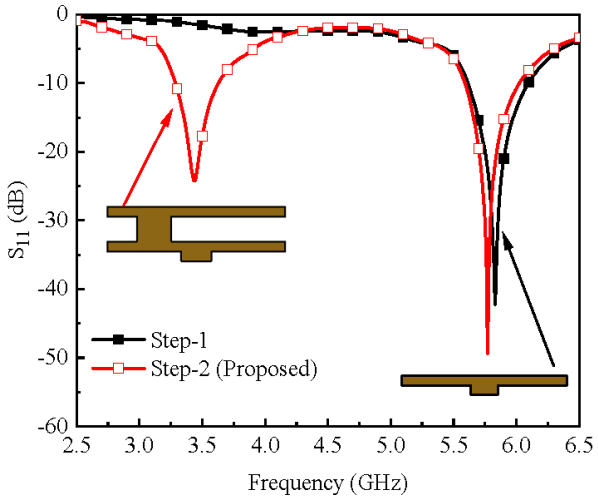

FIGURE 2. Reflection coefficient (S_{11}) of different design stages (inset of the figure shows design steps of the proposed single antenna element).

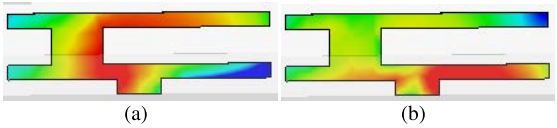

FIGURE 3. Surface current distribution of single antenna element at (a) 3.5 GHz and (b) 5.8 GHz.

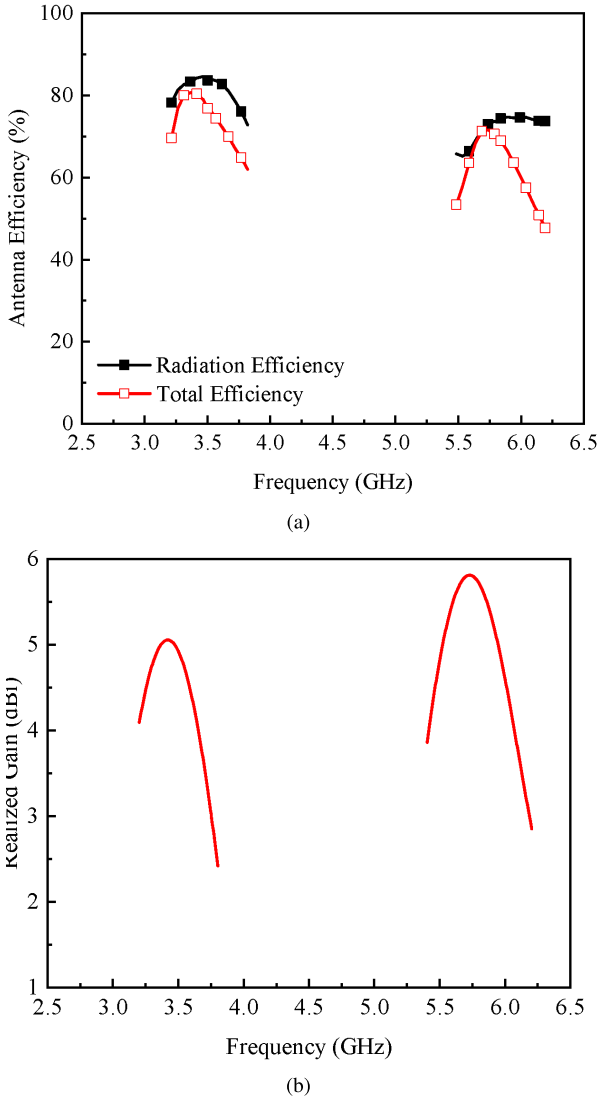

FIGURE 4. (a) Radiation and total efficiency, and (b) realized gain of single antenna element.

with the step-1 design (see inset of Figure 2). The addition of the stub and second strip provides a dual-band response at 3.5 GHz and 5.8 GHz frequency bands (see Figure 2, red curve). This effect may also be seen in Figure 3, which shows the surface current distribution for a single antenna element. One can observe from the result that for 3.5 GHz, a dense current is distributed on the top strip, stub, and in the center of the bottom strip, while for 5.8 GHz, the current is distributed on the surface of the bottom strip.

Figure 4(a) shows the simulated radiation and total efficiency of the proposed single antenna element. It can be seen that the radiation efficiency for 3.5 GHz and 5.8 GHz is $\geq$80% and >70%, respectively. On the other hand, the total efficiency for both bands is >60%. Moreover, the realized gain of a single antenna element is shown in Figure 4(b). The gain varies in the range of 2.5 dBi to 5 dBi for the 3.5 GHz frequency, while it varies in the range of 3-5.8 dBi for the 5.8 GHz frequency band. The simulated far-field radiation characteristics of the proposed single antenna element are shown in Figure 5. It is observed that the antenna offers a quasi-omnidirectional radiation pattern for both the frequency bands in *yz*- and *xz*-plane.

A parametric study was conducted to understand the behavior of a single antenna element. Two main variables, L_1 and L_2 are being investigated. For $L_1 = 10$ mm, the antenna has a single frequency response around 3.5 GHz (see Figure 6a). This value shifts around 4.75 GHz for $L_1 = 12$ mm and 14 mm, as shown in Figure 6(a). The antenna provides a dual-band response for values greater than 14 mm, and the desired results are obtained for $L_1 = 18$ mm, as shown in Figure 6(a). On the other hand, when the value of L_2 changed from 10 mm to 20 mm, the resonant frequencies shift from higher bands to lower bands (see Figure 6b). In case of L_2, the desired response is noted for a value of 18 mm, as shown

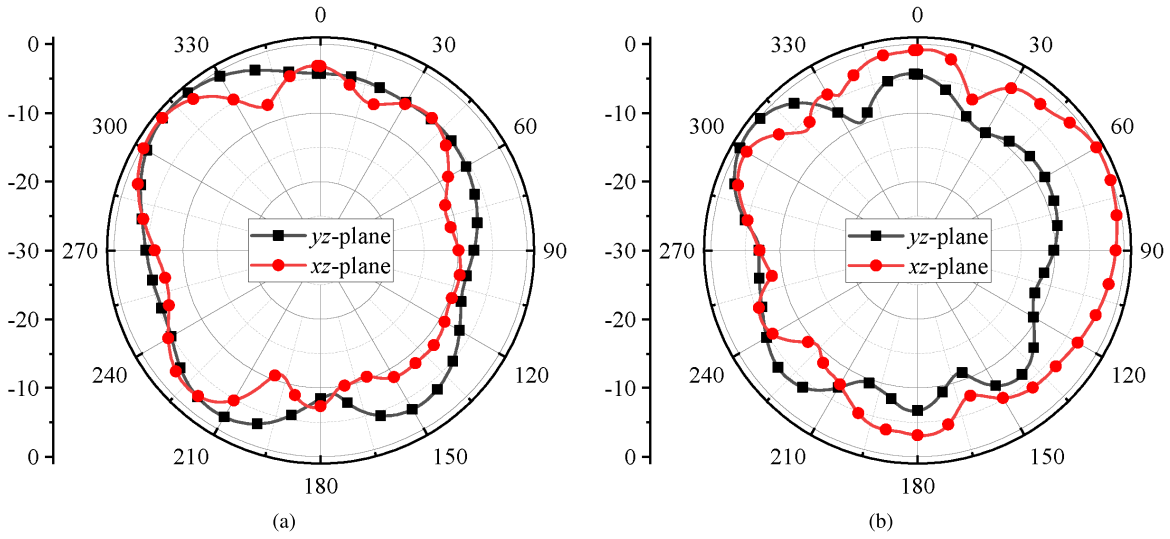

FIGURE 5. Simulated far-field radiation characteristics of single antenna element at (a) 3.5 GHz and (b) 5.8 GHz.

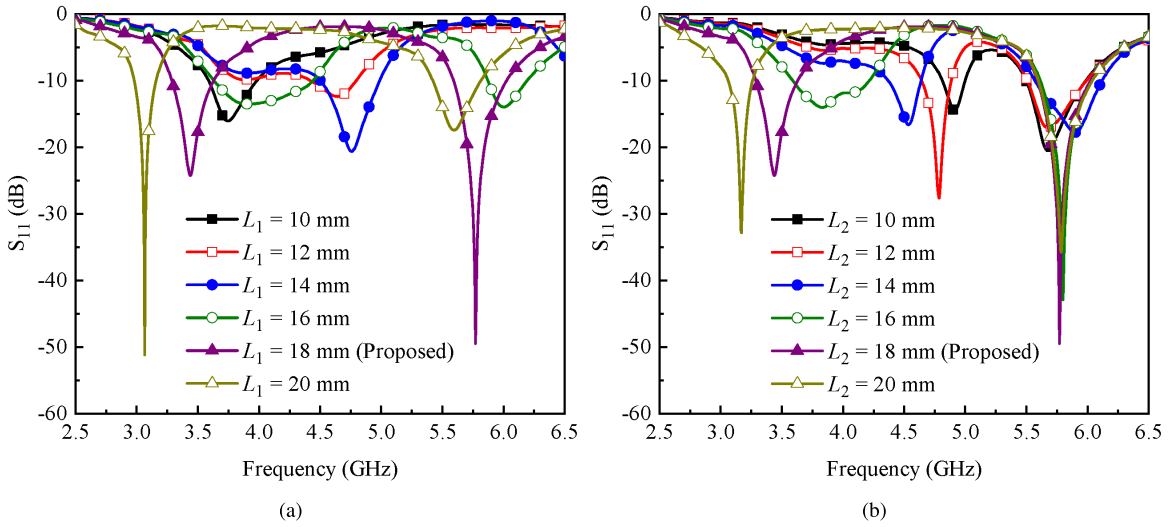

FIGURE 6. Effect of (a) L_1 and (b) L_2 on the performance of single antenna element.

in Figure 6(b). Therefore, from the presented results, one can tune the dual-band response at desired frequencies by changing the values of L_1 and L_2.

B. MIMO DESIGN

After analyzing the performance of a single antenna element, an eight-element MIMO array is constructed and analyzed. Figure 7(a) shows the perspective view of the proposed MIMO antenna system. One can note from the figure that the MIMO antenna consists of two sub-arrays of four radiating elements (see Figure 7b) printed on the side edge frame of the smartphone PCB. This technique provides space to accommodate batteries, liquid crystal devices (LCDs), radio frequency (RF) systems and subsystems, cameras, and sensor modules. The gap between each antenna element is optimized to achieve low mutual coupling. Furthermore, as shown in Figure 7(a), the sub-arrays are placed in two different planes, ensuring pattern diversity configuration. For the excitation of antenna elements, a 50Ω microstrip feeding line is used, and the signal is provided through a coaxial connector placed on the bottom side of the smartphone PCB (see Figure 7a). The remaining parameters are as follows: $L_{S1} = 150$, $W_{S1} = 7$, $S = 22$, and $g = 6$ (all dimensions in mm).

The simulated reflection coefficients of the proposed MIMO antenna are shown in Figure 8(a). Due to symmetry, the reflection coefficients of a single sub-array are shown. The results show that all the antenna elements resonate well for the desired frequency bands, i.e., 3.5 GHz and 5.8 GHz. According to the −6 dB bandwidth criteria, the observed impedance bandwidths for both bands are 680 MHz (3.1-3.78 GHz) and 780 MHz (5.43-6.21 GHz). Figure 8(b) depicts the isolation performance between the antenna

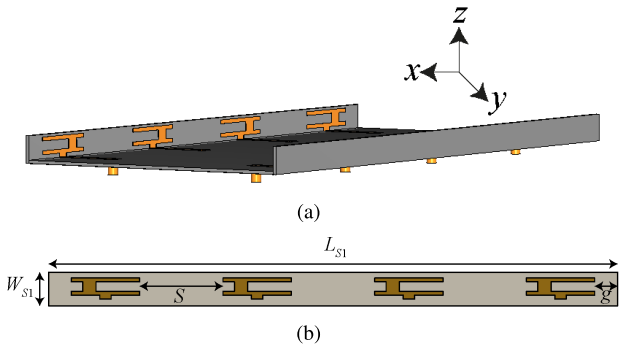

FIGURE 7. (a) Perspective view of proposed MIMO antenna system. (b) Design of single sub-array having four radiating elements.

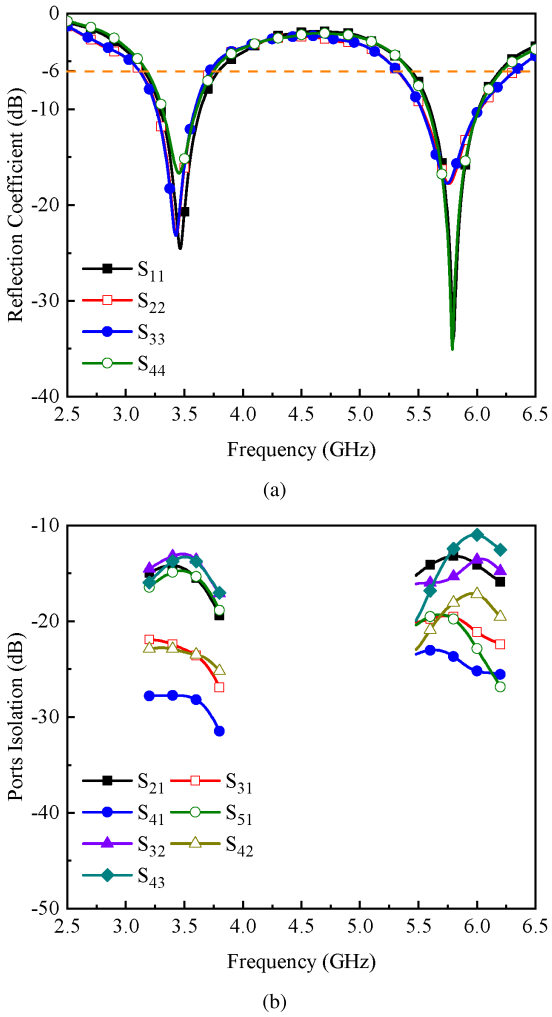

FIGURE 8. Simulated (a) reflection coefficients of MIMO antenna elements and (b) isolation between antenna elements.

elements. It can be seen that the isolation between adjacent antenna elements is >12 dB for 3.5 GHz and >10 dB for the 5.8 GHz frequency band. The maximum isolation is observed between antenna-1 and antenna-4, which is >25 dB and >20 dB for the 3.5 GHz and 5.8 GHz frequency bands, respectively.

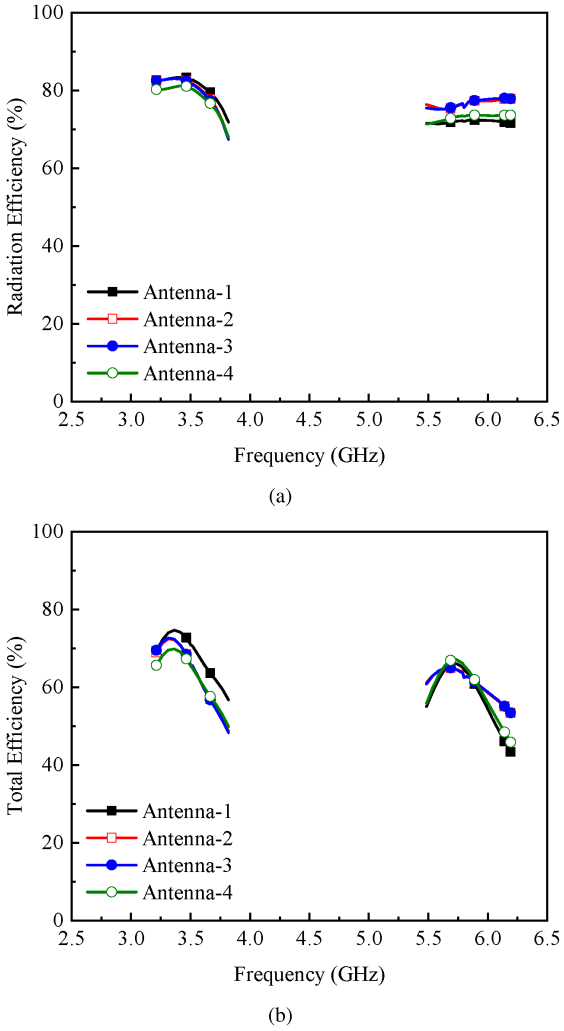

FIGURE 9. (a) Radiation and (b) total efficiencies of the proposed MIMO antenna system.

The MIMO antenna's simulated radiation and total efficiency for a single sub-array is shown in Figure 9. Both frequency bands have radiation efficiencies greater than 70% (see Figure 9a), while total efficiency varies between 50% and 78% for the 3.5 GHz frequency band and 42-70% for the 5.8 GHz frequency band, as shown in Figure 9(b).

III. FABRICATION AND MEASUREMENTS

The prototype of the proposed MIMO antenna is shown in Figure 10. A Precision Network Analyzer (PNA) E8363C from Agilent Technologies was used to measure the S-parameters. The measured reflection coefficients and port isolations are shown in Figure 11. As can be observed from Figure 11(a), the antenna elements are able to resonate in the frequency range of 3.1-3.9 GHz and 5.5-6.3 GHz. The measured −6 dB impedance bandwidth is observed to be 800 MHz for both the 3.5 GHz and 5.8 GHz frequency bands (see Figure 11a). Figure 11(b) shows the isolation between the antenna elements. The isolation between adjacent antenna elements is noted to be >12 dB

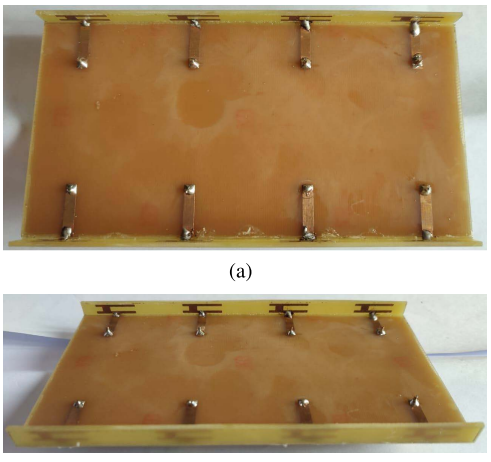

FIGURE 10. Fabricated prototype of the proposed MIMO antenna (a) front view (b) perspective view.

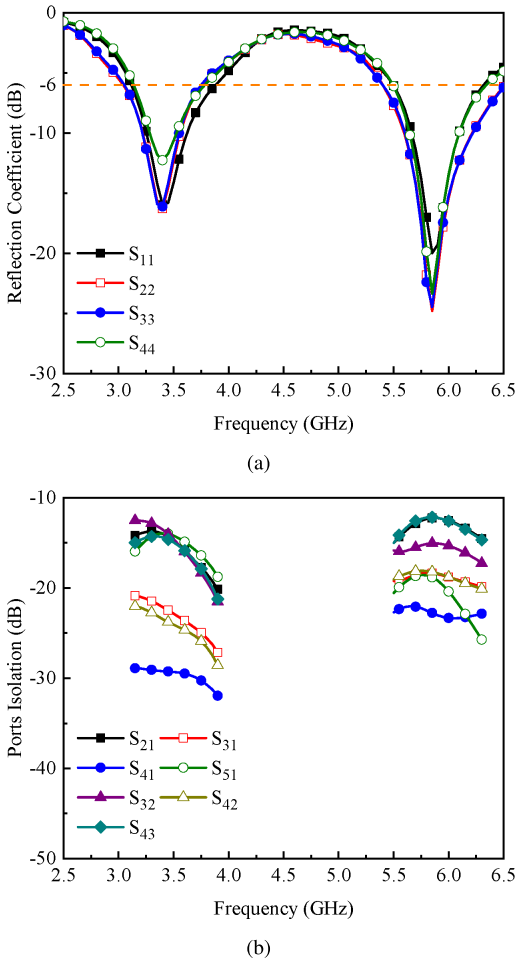

FIGURE 11. Measured (a) reflection coefficients of MIMO antenna elements and (b) isolation between antenna elements.

for both the frequency bands. The maximum isolation is observed between antenna-1 and antenna-4, which is >25 dB and >20 dB for the 3.5 GHz and 5.8 GHz frequency bands,

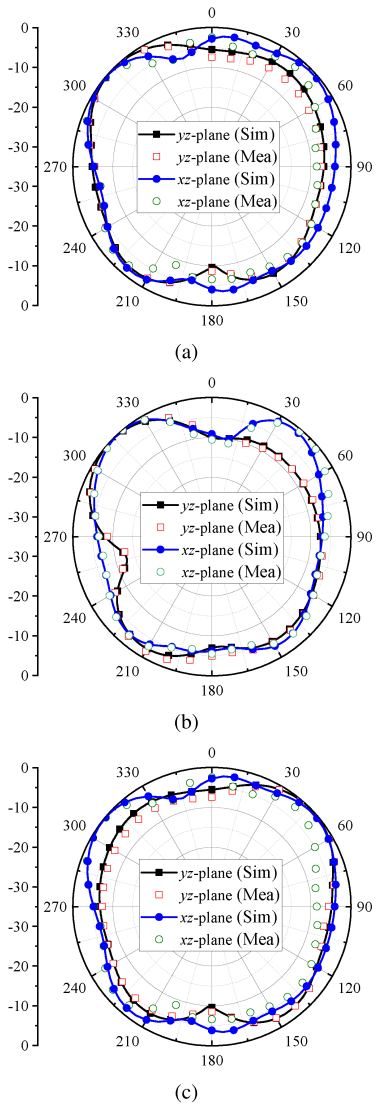

FIGURE 12. Simulated and measured far-field radiation characteristics of the proposed MIMO antenna at 3.5 GHz for (a) antenna-1, (b) antenna-2, and (c) antenna-5.

respectively. From Figure 11, some difference between the simulated (see Figure 8) and measured results is observed, which is due to manufacturing tolerances and losses in the measurement setup.

The far-field radiation characteristics of the presented MIMO antenna are assessed using a traditional method. As a reference antenna, a dual-ridge horn antenna with a frequency range of 1-18 GHz is employed, and the designed MIMO antenna is mounted on a turntable that is positioned on the opposite side. RF absorbers are used to cover the anechoic chamber's walls in order to eliminate reflections. Figures 12 and 13 depict the computed and measured radiation properties for antenna-1, antenna-2, and antenna-5 at resonant frequencies of 3.5 GHz and 5.8 GHz. Figures 12(a) and 12(c) show that, for the 3.5 GHz frequency band, antenna-1 and antenna-5 exhibit quasi-omnidirectional radiation characteristics in both the *yz*- and *xz*-planes. In case

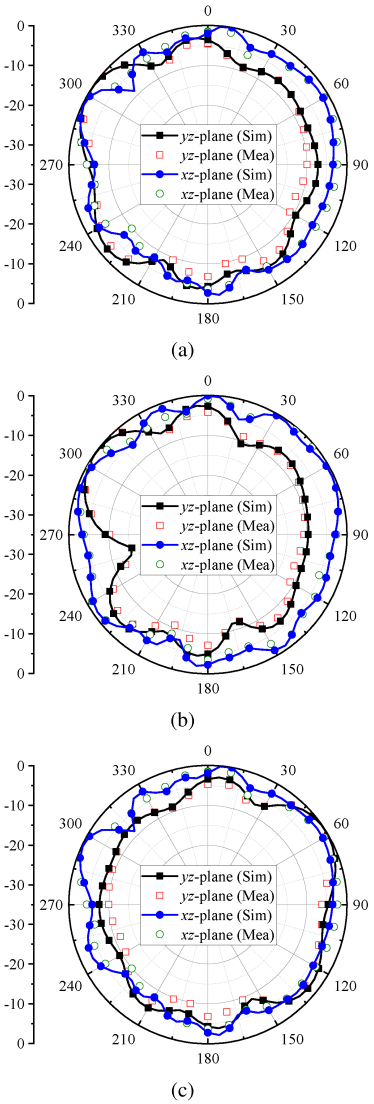

FIGURE 13. Simulated and measured far-field radiation characteristics of the proposed MIMO antenna at 5.8 GHz for (a) antenna-1, (b) antenna-2, and (c) antenna-5.

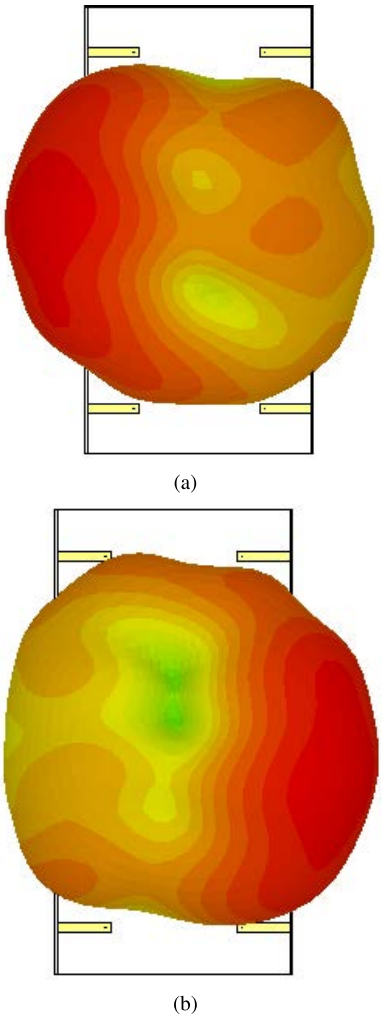

FIGURE 14. Simulated 3-D radiation patterns of the proposed MIMO antenna for (a) antenna-1 and (b) antenna-5.

of antenna-2, a butterfly like radiation pattern is observed for both the planes (see Figure 12b). It can also be observed from Figure 12(b) that the main beam for both the planes is directed towards 315°. Furthermore, from Figures 12(a) and 12(c), it is noted that antenna-1 and antenna-5 provide pattern diversity in both planes, which is a useful characteristic for modern smartphone applications.

In the 5.8 GHz frequency band, antenna-1, antenna-2, and antenna-5 provide quasi-omnidirectional radiation properties in both the *yz*- and *xz*-planes (see Figures 13a-c). In addition, just like in the 3.5 GHz frequency band, antenna-1 and antenna-5 provide pattern diversity in both planes, as shown in Figures 13(a) and 13(c). This effect can also be observed from the plot of Figure 14 where three-dimensional (3-D) radiation patterns of antenna-1 and antenna-5 are provided. From the result, one can clearly see that both the antenna elements are able to provide pattern diversity.

IV. DIVERSITY PERFORMANCE

In this section, a detailed description of the diversity performance of the designed MIMO antenna system is presented. The performance is assessed in terms of ECC, diversity gain (DG), and CC.

A. ENVELOPE CORRELATION COEFFICIENT (ECC)

ECC shows how effectively radiating elements are isolated within an array [22], [23]. It can be expressed as [24], [25] (1), as shown at the bottom of the next page, where M_a and M_b represent far-field characteristics of port a and port b.

It has been described that the value of ECC should be <0.5 for practical applications [26]. From Figure 15(a), it is observed that for the proposed MIMO antenna, the simulated value of ECC for both the frequency bands is less than 0.035, while the measured values are noted to be less than 0.1 and 0.12 for the 3.5 GHz and 5.8 GHz frequency bands, respectively, as shown in Figure 15(b). This result indicates that the interference between the elements is minimal.

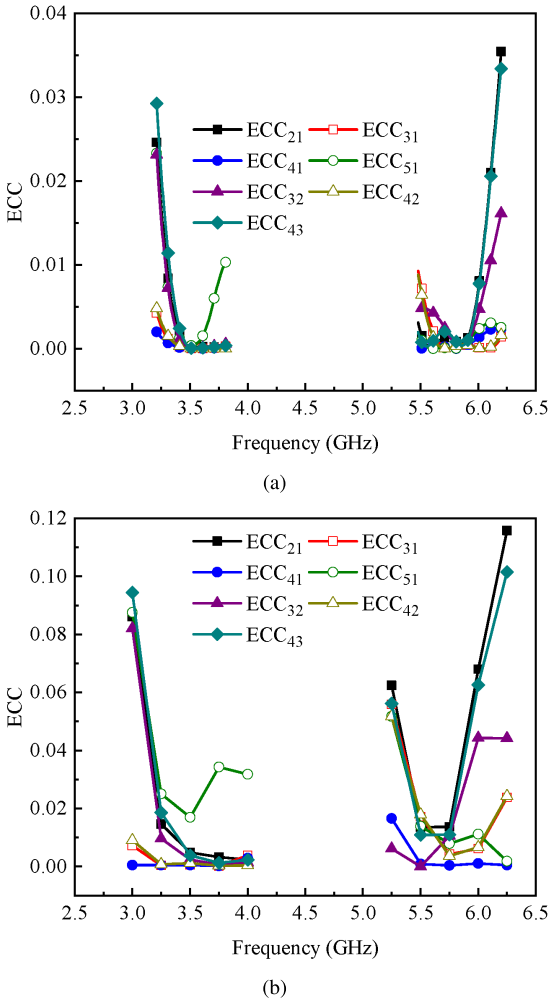

FIGURE 15. Envelope correlation coefficient of the proposed MIMO antenna (a) simulated (b) measured.

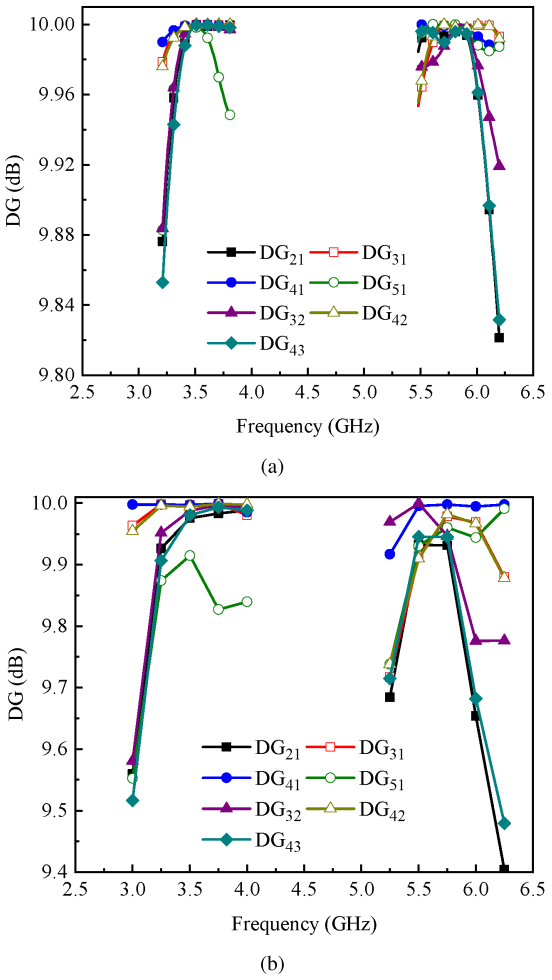

FIGURE 16. Diversity gain of the proposed MIMO antenna (a) simulated (b) measured.

B. DIVERSITY GAIN (DG)

Another important feature that needs to be assessed is DG. The DG of the MIMO antennas should be high (≈10 dB) in the operating bandwidth. It is expressed in terms of ECC as [24]:

$$\mathrm{DG} = 10\sqrt{1 - \mathrm{ECC}^2} \tag{2}$$

Figure 16 depicts the DG of the proposed MIMO antenna. The simulated value of DG for both frequency bands is >9.8 dB (see Figure 16a), whereas the measured value is >9.4 dB (see Figure 16b).

C. CHANNEL CAPACITY (CC)

The ergodic CC of the proposed MIMO antenna is shown in Figure 17. It is evaluated by averaging 10,000 realizations of Rayleigh fading with a reference signal-to-noise ratio (SNR) of 20 dB [27]. Mathematically, the CC of any MIMO system can be calculated using the expression mentioned in [23]. For our proposed MIMO antenna, the value of CC lies in the range of 36-41 bps/Hz for both the frequency bands (see Figure 17), which is very close to the ideal value [28].

A comparison among proposed and previously presented MIMO antennas is presented in Table 1. From the data in the table, it is observed that the proposed MIMO antenna offers high efficiency compared to the designs presented in [5]–[11], [14], [17], and [19]. In addition, the presented MIMO antenna provides low ECC compared to the designs of [5], [8], [9], [11], and [17], which tend to achieve high CC in the bands of interest.

$$\mathrm{ECC} = \left| \frac{\iint_{4\pi} M_a(\theta,\phi).M_b^*(\theta,\phi)d\Omega}{\sqrt{\iint_{4\pi} M_a(\theta,\phi).M_a^*(\theta,\phi)d\Omega \iint_{4\pi} M_b(\theta,\phi).M_b^*(\theta,\phi)d\Omega}} \right|^2 \tag{1}$$

TABLE 1. Comparison among proposed and previously reported MIMO antennas.

Ref.	Board Size (mm^2)	No. of Elements	Frequency Band (GHz)	Efficiency (%)	Isolation (dB)	ECC
[5]	150×80	10	3.5/5.5	65/80	>15	<0.15
[6]	150×80	8	3.4-3.6	>62	>17	<0.05
[7]	150×73	8	3.4-3.6	61	>17	<0.07
[8]	150×73	4	3.4-3.6	30-50	>17	<0.1
[9]	150×75	8	3.3-6	>40	>10	<0.12
[10]	150×75	8	2.5-3.6	65	>13	<0.02
[11]	124×74	8	3.3-3.6	40	>15	<0.15
[12]	150×75	8	3.2-4	80	20	<0.01
[13]	150×75	8	3.3-3.9	60-80	18	<0.005
[14]	150×75	8	3.4-3.6	70	>15	<0.0125
[17]	150×75	8	3.25-3.82/4.79-6.2	60-70	>10.5	<0.12
[19]	150×75	8	2.46-2.65/3.4-3.7/5.6-6	>60	>10	<0.01
[21]	150×75	8	3.4-4.4	>90	>16	<0.005
This Work	150×75	8	3.1-3.9/5.5-6.3	70-80	>12	<0.035

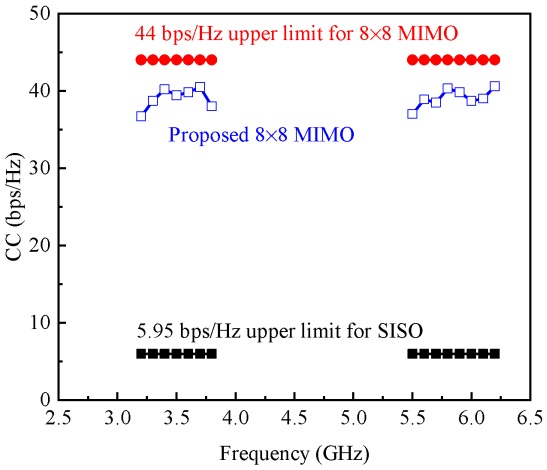

FIGURE 17. Channel capacity of the proposed MIMO antenna.

V. CONCLUSION

This work presents the design of an eight-element dual-band MIMO antenna system for sub-6 GHz 5G technology. The MIMO's single antenna element is composed of an H-shaped radiator designed on the side edge frame of the smartphone, while each side edge has four elements. It is observed that the antenna elements resonate around the 3.5 GHz and 5.8 GHz frequency bands. The bandwidth of the radiating elements is noted to be 680 MHz (3.1-3.78 GHz) and 780 MHz (5.43-6.21 GHz). Furthermore, >12 dB of isolation is noted between MIMO elements, which led to achieving low ECC, high DG, and high CC. From the presented results, it can be concluded that the proposed MIMO antenna system is suitable for 5G-enabled smartphones.

REFERENCES

[1] N. Hussain, M.-J. Jeong, A. Abbas, and N. Kim, "Metasurface-based single-layer wideband circularly polarized MIMO antenna for 5G millimeter-wave systems," *IEEE Access*, vol. 8, pp. 130293–130304, 2020.

[2] M. Ikram, N. Nguyen-Trong, and A. M. Abbosh, "Common-aperture sub-6 GHz and millimeter-wave 5G antenna system," *IEEE Access*, vol. 8, pp. 199415–199423, 2020.

[3] J. Dong, S. Wang, and J. Mo, "Design of a twelve-port MIMO antenna system for multi-mode 4G/5G smartphone applications based on characteristic mode analysis," *IEEE Access*, vol. 8, pp. 90751–90759, 2020.

[4] N. Kumar and R. Khanna, "A two element MIMO antenna for sub-6 GHz and mmWave 5G systems using characteristics mode analysis," *Microw. Opt. Technol. Lett.*, vol. 63, no. 2, pp. 587–595, Feb. 2021.

[5] Y. Li, C.-Y.-D. Sim, Y. Luo, and G. Yang, "Multiband 10-antenna array for sub-6 GHz MIMO applications in 5-G smartphones," *IEEE Access*, vol. 6, pp. 28041–28053, 2018.

[6] Y. Li, C.-Y.-D. Sim, Y. Luo, and G. Yang, "High-isolation 3.5 GHz eight-antenna MIMO array using balanced open-slot antenna element for 5G smartphones," *IEEE Trans. Antennas Propag.*, vol. 67, no. 6, pp. 3820–3830, Jun. 2019.

[7] L. B. Sun, H. Feng, Y. Li, and Z. Zhang, "Compact 5G MIMO mobile phone antennas with tightly arranged orthogonal-mode pairs," *IEEE Trans. Antennas Propag.*, vol. 66, no. 11, pp. 6364–6369, Nov. 2018.

[8] Z. Ren, A. Zhao, and S. Wu, "MIMO antenna with compact decoupled antenna pairs for 5G mobile terminals," *IEEE Antennas Wireless Propag. Lett.*, vol. 18, no. 7, pp. 1367–1371, Jul. 2019.

[9] X. Zhang, Y. Li, W. Wang, and W. Shen, "Ultra-wideband 8-port MIMO antenna array for 5G metal-frame smartphones," *IEEE Access*, vol. 7, pp. 72273–72282, 2019.

[10] M. Abdullah, S. H. Kiani, and A. Iqbal, "Eight element multiple-input multiple-output (MIMO) antenna for 5G mobile applications," *IEEE Access*, vol. 7, pp. 134488–134495, 2019.

[11] W. Jiang, B. Liu, Y. Cui, and W. Hu, "High-isolation eight-element MIMO array for 5G smartphone applications," *IEEE Access*, vol. 7, pp. 34104–34112, 2019.

[12] N. O. Parchin, H. J. Basherlou, M. Alibakhshikenari, Y. O. Parchin, Y. I. A. Al-Yasir, R. A. Abd-Alhameed, and E. Limiti, "Mobile-phone antenna array with diamond-ring slot elements for 5G massive MIMO systems," *Electronics*, vol. 8, no. 5, p. 521, May 2019.

[13] N. O. Parchin, Y. I. A. Al-Yasir, H. J. Basherlou, R. A. Abd-Alhameed, and J. M. Noras, "Orthogonally dual-polarised MIMO antenna array with pattern diversity for use in 5G smartphones," *IET Microw., Antennas Propag.*, vol. 14, no. 6, pp. 457–467, May 2020.
[14] A. Zhao and Z. Ren, "Size reduction of self-isolated MIMO antenna system for 5G mobile phone applications," *IEEE Antennas Wireless Propag. Lett.*, vol. 18, no. 1, pp. 152–156, Jan. 2019.
[15] A. Zhao, Z. Ren, and S. Wu, "Broadband MIMO antenna system for 5G operations in mobile phones," *Int. J. RF Microw. Comput.-Aided Eng.*, vol. 29, no. 10, Oct. 2019, Art. no. e21857.
[16] A. Zhao and Z. Ren, "Multiple-input and multiple-output antenna system with self-isolated antenna element for fifth-generation mobile terminals," *Microw. Opt. Technol. Lett.*, vol. 61, no. 1, pp. 20–27, 2019.
[17] H. Wang, R. Zhang, Y. Luo, and G. Yang, "Compact eight-element antenna array for triple-band MIMO operation in 5G mobile terminals," *IEEE Access*, vol. 8, pp. 19433–19449, 2020.
[18] N. O. Parchin, H. J. Basherlou, Y. I. A. Al-Yasir, and R. A. Abd-Alhameed, "A broadband multiple-input multiple-output loop antenna array for 5G cellular communications," *AEU, Int. J. Electron. Commun.*, vol. 127, Dec. 2020, Art. no. 153476.
[19] N. Ojaroudi Parchin, H. Jahanbakhsh Basherlou, and R. A. Abd-Alhameed, "Design of multi-mode antenna array for use in next-generation mobile handsets," *Sensors*, vol. 20, no. 9, p. 2447, Apr. 2020.
[20] N. O. Parchin, Y. I. A. Al-Yasir, A. M. Abdulkhaleq, H. J. Basherlou, A. Ullah, and R. A. Abd-Alhameed, "A new broadband MIMO antenna system for sub 6 GHz 5G cellular communications," in *Proc. 14th Eur. Conf. Antennas Propag. (EuCAP)*, Mar. 2020, pp. 1–4.
[21] N. Ojaroudi Parchin, H. Jahanbakhsh Basherlou, Y. I. A. Al-Yasir, A. M. Abdulkhaleq, M. Patwary, and R. A. Abd-Alhameed, "A new CPW-fed diversity antenna for MIMO 5G smartphones," *Electronics*, vol. 9, no. 2, p. 261, Feb. 2020.
[22] U. Ahmad, S. Ullah, U. Rafique, D.-Y. Choi, R. Ullah, B. Kamal, and A. Ahmad, "MIMO antenna system with pattern diversity for sub-6 GHz mobile phone applications," *IEEE Access*, vol. 9, pp. 149240–149249, 2021.
[23] R. Ullah, S. Ullah, F. Faisal, R. Ullah, I. B. Mabrouk, M. J. Al Hasan, and B. Kamal, "A novel multi-band and multi-generation (2G, 3G, 4G, and 5G) 9-elements MIMO antenna system for 5G smartphone applications," *Wireless Netw.*, vol. 27, pp. 4825–4837, Sep. 2021.
[24] S. Agarwal, U. Rafique, R. Ullah, S. Ullah, S. Khan, and M. Donelli, "Double overt-leaf shaped CPW-fed four port UWB MIMO antenna," *Electronics*, vol. 10, no. 24, p. 3140, Dec. 2021.
[25] A. G. Alharbi, U. Rafique, S. Ullah, S. Khan, S. M. Abbas, E. M. Ali, M. Alibakhshikenari, and M. Dalarsson, "Novel MIMO antenna system for ultra wideband applications," *Appl. Sci.*, vol. 12, no. 7, p. 3684, 2022.
[26] M. Koohestani, A. A. Moreira, and A. K. Skrivervik, "A novel compact CPW-fed polarization diversity ultrawideband antenna," *IEEE Antennas Wireless Propag. Lett.*, vol. 13, pp. 563–566, 2014.
[27] M. Abdullah, S. H. Kiani, L. F. Abdulrazak, A. Iqbal, M. A. Bashir, S. Khan, and S. Kim, "High-performance multiple-input multiple-output antenna system for 5G mobile terminals," *Electronics*, vol. 8, no. 10, p. 1090, Sep. 2019.
[28] Y. Li, H. Zou, M. Wang, M. Peng, and G. Yang, "Eight-element MIMO antenna array for 5G/sub-6 GHz indoor micro wireless access points," in *Proc. Int. Workshop Antenna Technol. (iWAT)*, 2018, pp. 1–4.

MUHAMMAD NOAMAN ZAHID received the M.S. degree from the Capital University of Science & Technology (CUST), Pakistan, in 2015. He is a Postgraduate Researcher and a Technical Expert (TE) with the Hunan University of Humanities, Science and Technology, located in the southern part of China. His research interests include RF circuit designing, fabrication for wireless and RFID applications, and electromagnetics and optical communication.

ZHU GAOFENG was born in 1979. He received the Ph.D. degree in control science and control engineering from Central South University. He is an Associate Professor of electronics. His research interests include in photoelectric detection technology and computer control technology.

SAAD HASSAN KIANI (Graduate Student Member, IEEE) received the bachelor's degree in electrical engineering (telecommunication) from the City University of Science and Information Technology (CUSIT), in 2014, and the M.Sc. degree in electrical engineering from Iqra National University (IN) from Peshawar, Pakistan, in 2018. He is pursuing the Ph.D. degree in electrical engineering with IIC University of Technology, Phnom Penh, Cambodia. He was a Lecturer at CUSIT and an Adjunct Faculty member at Iqra National University. He is also a visiting Ph.D. Researcher at Prince Sultan University, Saudi Arabia. His research interests include MIMO antenna designs, 5G antennas, mm-wave antennas, isolation enhancement among MIMO antenna elements, and origami and kirigami antennas.

UMAIR RAFIQUE (Graduate Student Member, IEEE) received the B.S. degree in electronic engineering from Mohammad Ali Jinnah University (MAJU), Islamabad Campus, Karachi, Pakistan, in 2011, and the M.S. degree in electronic engineering from the Capital University of Science and Technology (CUST), Islamabad, Pakistan, in 2017. Currently, he is pursuing a Ph.D. degree in applied electromagnetics with the Sapienza University of Rome, Rome, Italy. From June 2010 to January 2012, he was a Research Associate at the Research Group of Microelectronics and FPGAs at MAJU. From May 2013 to March 2015, he was an RF Design Engineer at AKSA Solutions Development Services (AKSA-SDS), where he was responsible for the design, development, and implementation of RF front-ends for airborne and military applications. From October 2015 to May 2021, he was a Research Associate at the Research Group of Microelectronics and RF Engineering at CUST. He also worked as a Freelancer with Meshtech AS, a Norway-based organization, from August 2016 to August 2017, where he was responsible for designing onboard antennas and bandpass filters for WLAN applications. His research interests include MIMO antennas for sub-6 GHz and mm-wave applications; UWB and SWB antennas; frequency selective surfaces; metamaterials and metasurfaces; RF front-ends and circuits; near-field microwave imaging; electronic system design and integration; and semiconductor device modeling. He has published a number of research articles in reputed international journals and conferences, and holds a research impact factor of 35.192 with a citation index of 269. He is a Graduate Student Member of IEEE Antennas and Propagation Society (IEEE APS), USA; IEEE Microwave Theory and Techniques Society (IEEE MTTS), USA; and a Registered Engineer with the Pakistan Engineering Council (PEC). He also acts as a referee in several highly reputed journals.

SYED MUZAHIR ABBAS (Senior Member, IEEE) received the B.Sc. degree in electrical (telecommunication) engineering from the COMSATS Institute of Information Technology (CIIT), Islamabad, Pakistan, in 2006, the M.Sc. degree in computer engineering from the Center for Advanced Studies in Engineering (CASE), Islamabad, in 2009, and the Ph.D. degree in electronics engineering at Macquarie University, North Ryde, N.S.W., Australia, in 2016. He is a Transmission Engineer with Alcatel-Lucent, Pakistan, a RF Engineer with CommScope, Australia, and a Senior Antenna Design Engineer with Benelec Technologies, Australia. He has lectured various courses at CIIT, Islamabad, Pakistan, and in Australia with Western Sydney University, Macquarie University and University of Sydney. Currently, he is working as the Senior Principal Engineer with Benelec Technologies, Australia. He has been a Visiting Researcher with the ElectroScience Laboratory, Ohio State University, USA, and the Queen Mary University of London, U.K. He has also received several prestigious awards and fellowships, including the 2020 IEEE 5G World Forum Best Paper Award, the 2019 IEEE NSW Outstanding Young Professional Award, the 2018 Young Scientist Award (Commission B-Field and Waves) from the International Union of Radio Science (URSI), the 2013 CSIRO Postgraduate Fellowship, the 2012 iMQRES Award for Ph.D., and the Research Productivity Awards in 2012 and 2010 from CIIT, Pakistan. His research interests include base station antennas, mmWave antennas, high-impedance surfaces, frequency selective surfaces, flexible/embroidered antennas, CNT yarns, CNT/graphene-based antennas, reconfigurable antennas/electronics, and the development of antennas for UWB and WBAN applications.

MOHAMMAD ALIBAKHSHIKENARI (Member, IEEE) was born in Mazandaran, Iran, in February 1988. He received the Ph.D. degree (Hons.) with European Label in electronics engineering from the University of Rome ''Tor Vergata'', Italy, in February 2020. He was a Ph.D. Visiting Researcher at the Chalmers University of Technology, Sweden, in 2018. His training during the Ph.D. included a research stage in the Swedish company Gap Waves AB. He is currently with the Department of Signal Theory and Communications, Universidad Carlos III de Madrid (uc3m), Spain, as the Principal Investigator of the CONEX-Plus Talent Training Program and Marie Sklodowska-Curie Actions. He is also a Lecturer of the electromagnetic fields and electromagnetic laboratory with the Department of Signal Theory and Communications. His research interests include electromagnetic systems, antennas and wave-propagations, metamaterials and metasurfaces, synthetic aperture radars (SAR), multiple-input multiple output (MIMO) systems, RFID tag antennas, substrate integrated waveguides (SIWs), impedance matching circuits, microwave components, millimeter-waves and terahertz integrated circuits, gap waveguide technology, beamforming matrix, and reconfigurable intelligent surfaces (RIS). The above research lines have produced more than 200 publications on international journals, presentations within international conferences, and book chapters with a total number of the citations more than 3300 and H-index of 40 reported by Google Scholar. He was a recipient of the three years research grant funded by Universidad Carlos III de Madrid and the European Union's Horizon 2020 Research and Innovation Program under the Marie Sklodowska-Curie Grant in July 2021, the two years research grant funded by the University of Rome ''Tor Vergata'' started in November 2019, the three years Ph.D. Scholarship funded by the University of Rome ''Tor Vergata'' started in November 2016, and the two Young Engineer Awards of the 47th and 48th European Microwave Conference held in Nuremberg, Germany, in 2017, and in Madrid, Spain, in 2018, respectively. For academic year 2021–2022, he received the ''Teaching Excellent Acknowledgement'' Certificate for the course of electromagnetic fields from Vice-Rector of studies of uc3m. His research article entitled ''High-Gain Metasurface in Polyimide On-Chip Antenna Based on CRLH-TL for Sub Terahertz Integrated Circuits'' published in Scientific Reports was awarded as the Best Month Paper at the University of Bradford, U.K., in April 2020. He is serving as an Associate Editor for *IET Journal of Engineering* and *International Journal of Antennas and Propagation*. He also acts as a referee in several highly reputed journals and international conferences.

MARIANA DALARSSON (Member, IEEE) received the M.Sc. degree in physics and the Ph.D. degree in electromagnetic theory from the KTH Royal Institute of Technology, Stockholm, Sweden, in 2010 and 2016, respectively, and the Docent degree from the Linnaeus University, Växjö, Sweden. She received the Honorary Grant given to the best graduate of the year of her M.Sc. programme, in 2011. She is also the second youngest woman ever to be awarded a Ph.D. degree from KTH. From 2016 to 2019, she was a Postdoctoral Researcher at the Group of Waves, Signals and Systems, Linnaeus University. From 2019 to 2020, she was an Assistant Professor at the Department of Electrical and Information Technology, Lund University, Lund, Sweden. Currently, she is an Assistant Professor with the KTH Royal Institute of Technology. She is the author of more than 80 scientific publications, including 40 journal articles and one book. Her teaching and research interests include electromagnetic scattering and absorption, inverse problems, electromagnetics of stratified media, double-negative metamaterials, and mathematical physics. Currently, she is mainly pursuing research as PI within her own project grant ''Waveguide Theory for Artificial Materials and Plasmonics'' awarded by the Swedish Research Council. She is the winner of multiple teaching and research awards, including the L'Oréal-Unesco for Women in Science Sweden Award in 2021.